Journal of Pathology
J Pathol 2021; **00:** 000–000
Published online 27 August 2021 in Wiley Online Library (wileyonlinelibrary.com) DOI: 10.1002/path.5770

ORIGINAL PAPER

Clinical ApoA-IV amyloid is associated with fibrillogenic signal sequence

Diana Canetti[1], Paola Nocerino[1], Nigel B Rendell[1], Nicola Botcher[2], Janet A Gilbertson[2], Angel Blanco[2], Dorota Rowczenio[2], Alessandra Morelli[3], P Patrizia Mangione[1,3], Alessandra Corazza[4], Guglielmo Verona[1], Sofia Giorgetti[3], Loredana Marchese[3], Per Westermark[5], Philip N Hawkins[2], Julian D Gillmore[2], Vittorio Bellotti[1,3] and Graham W Taylor[1]*

[1] *Wolfson Drug Discovery Unit, Centre for Amyloidosis and Acute Phase Proteins, Division of Medicine, University College London, London, UK*
[2] *National Amyloidosis Centre, University College London and Royal Free Hospital, London, UK*
[3] *Department of Molecular Medicine, Institute of Biochemistry, University of Pavia, Pavia, Italy*
[4] *Department of Medicine (DAME), University of Udine, Udine, Italy*
[5] *Department of Immunology, Genetics and Pathology, Uppsala University, Uppsala, Sweden*

**Correspondence to: GW Taylor, Wolfson Drug Discovery Unit and National Amyloidosis Centre, Centre for Amyloidosis and Acute Phase Proteins, Division of Medicine, University College London, Royal Free Campus, Rowland Hill Street, London NW3 2PF, UK. E-mail: graham.taylor@ucl.ac.uk*

Abstract

Apolipoprotein A-IV amyloidosis is an uncommon form of the disease normally resulting in renal and cardiac dysfunction. ApoA-IV amyloidosis was identified in 16 patients attending the National Amyloidosis Centre and in eight clinical samples received for histology review. Unexpectedly, proteomics identified the presence of ApoA-IV signal sequence residues (p.18-43 to p.20-43) in 16/24 trypsin-digested amyloid deposits but in only 1/266 non-ApoA-IV amyloid samples examined. These additional signal residues were also detected in the cardiac sample from the Swedish patient in which ApoA-IV amyloid was first described, and in plasma from a single cardiac ApoA-IV amyloidosis patient. The most common signal-containing peptide observed in ApoA-IV amyloid, p.20-43, and to a far lesser extent the N-terminal peptide, p.21-43, were fibrillogenic *in vitro* at physiological pH, generating Congo red-positive fibrils. The addition of a single signal-derived alanine residue to the N-terminus has resulted in markedly increased fibrillogenesis. If this effect translates to the mature circulating protein *in vivo*, then the presence of signal may result in preferential deposition as amyloid, perhaps acting as seed for the main circulating native form of the protein; it may also influence other ApoA-IV-associated pathologies.

Keywords: ApoA-IV amyloidosis; ApoA-IV sequence coverage; ApoA-IV signal-containing peptide; amyloid proteomics; targeted mass spectrometry in serum; fibrillogenic ApoA-IV signal-containing peptide

Received 10 March 2021; Revised 1 July 2021; Accepted 27 July 2021

No conflicts of interest were declared.

Introduction

Amyloidosis occurs when a diverse range of normal circulating proteins misfold and subsequently deposit as insoluble fibrillary masses in a range of tissues, resulting in organ dysfunction and clinical disease [1]. There are over 30 known amyloidogenic proteins associated with human disease [2]. Amyloid deposits can be restricted to specific organs – for example, fibrinogen Aα amyloid is invariably found in the kidney [3]; with other amyloidogenic proteins, such as transthyretin (TTR) or immunoglobulin light chains, amyloid can be detected in multiple organs [4–7]. In some cases, the development of the disease is associated with increased circulating concentrations of the precursor proteins, common examples being the kappa and lambda light chains arising from a monoclonal gammopathy [8] and serum amyloid A, which is associated with a raised inflammatory response [9]. With other proteins, including lysozyme, TTR, and fibrinogen Aα, the presence of a variant can result in protein destabilisation and the subsequent formation of amyloid [10–12]. Amyloid deposits can also arise from normal circulating levels of wild-type proteins. This is notable in the case of TTR, where amyloid deposits of wild-type protein are commonly found in the hearts of the elderly [13,14], possibly as a result of age-related oxidative changes [15]. Apolipoprotein A-IV (ApoA-IV) was originally identified as a new amyloid fibril protein in fibrils extracted from cardiac tissue of a patient with senile systemic

amyloidosis [now termed ATTR wild-type (ATTRwt) amyloidosis] [16]. Additional biochemical studies showed that the amyloidogenicity of ApoA-IV resided in the N-terminus. It was later shown by the same group that ApoA-IV and TTR were not co-deposited but occupied anatomically distinct regions, demonstrating that two types of amyloid can be present, and separately deposited, in the same tissue [17]. There were few further reports of ApoA-IV amyloid (AApoA-IV) since typing relied mainly on immunological techniques and few pathology laboratories had access to the original high-quality antibody for typing.

The observation that a mass spectrometric-based proteomics approach could be applied to identify proteins in formalin-fixed, paraffin-embedded (FFPE) material [18–21] led to the development of proteomics as a clinical service for typing amyloid by Ahmet Dogan and colleagues at the Mayo Clinic [22–25]. Proteomics makes it relatively easy to identify (and potentially quantify) any of the currently known amyloidogenic proteins in clinical samples. It was then determined by the Mayo team that ApoA-IV was a common constituent of amyloid deposits and could be used as a signature protein, together with serum amyloid P component and apolipoprotein E, to identify the presence of amyloid [24]. Whilst this was beneficial in typing amyloid by proteomics, it caused some difficulty in the identification of ApoA-IV as an amyloid protein rather than an amyloid-associated signature protein. Proteomics was used successfully at the Mayo Clinic to identify cases of renal and cardiac ApoA-IV amyloidosis [26–29]. This was based primarily on an unusual clinical presentation coupled with a high number of ApoA-IV peptides identified by proteomics (spectral count) and the absence of other obvious amyloidogenic proteins. These became their new criteria for identifying ApoA-IV amyloid. In our centre, we have developed further criteria for the identification of ApoA-IV amyloid based on clinical presentation together with morphological, immunohistochemical, and proteomics behaviour. We have also identified peptides containing signal sequence (p.18-43, p.19-43, and p.20-43) in a number of clinical ApoA-IV amyloid samples, suggesting that this may influence amyloid deposition and also be of diagnostic value in identifying this rare form of amyloidosis.

Materials and methods

Ethical approval

Samples were collected and analysed as part of routine clinical examination. Informed consent was obtained from all patients and clinical care was in accordance with the Declaration of Helsinki. The material collection and use for the original Swedish sample (#25) were performed under a valid permit by the Ethics Committee at Uppsala University Hospital (Ups 01-083).

Patients and samples

Fifteen patients with renal or cardiac dysfunction attending the UK NHS National Amyloidosis Centre (NAC) clinics between March 2016 and October 2020 were diagnosed with ApoA-IV amyloidosis (Table 1). Duodenal ApoA-IV amyloidosis was also diagnosed in a single patient. Samples of FFPE tissue or fat aspirates were obtained as part of routine diagnostic procedures and were evaluated as previously reported using Congo red staining, immunohistochemistry (IHC) with a panel of antibodies, and proteomics analysis [30–32]. Serum was prepared from blood taken from two healthy volunteers and from three patients given an AApoA-IV diagnosis. Eight tissue samples sent for histology review were also diagnosed with ApoA-IV amyloid based on IHC and the proteomics criteria. The FFPE block from the original patient diagnosed with ApoA-IV amyloidosis [16] was obtained from the Department of Immunology, Genetics and Pathology, Uppsala, Sweden and was recut to obtain 6-µm sections which were stained with Congo red, followed by IHC using an anti-TTR antibody [33] and an anti-ApoA-IV antipeptide antibody [17]. Two separate areas of TTR-positive and ApoA-IV-positive amyloid were micro-dissected and captured.

Proteomics analysis

Full experimental details of our proteomics approach, based on that of the Mayo Clinic, have been reported previously [34]. Samples were originally analysed on a Thermo Velos Orbitrap mass spectrometer coupled to a Waters nanoACQUITY UPLC system and, more recently, on a Thermo Q-Exactive Plus mass spectrometer (Thermo Fisher Scientific, Bremen, Germany) coupled to a Dionex Ultimate 3000 UPLC system (Thermo Fisher Scientific). Data were analysed by Mascot software (Matrix Science, London, UK) using the Swiss-Prot human database. Search parameters were charge states +2, +3, and +4; precursor mass tolerance of 10 ppm; and 0.6 Da for HCD fragments; the more intense ^{13}C ion was normally selected for dissociation. Trypsin was used as the *in silico* proteolytic enzyme, with semi-trypsin included to identify additional non-tryptic signal sequences. The significance level was set at $p < 0.05$. Methionine oxidation was included as variable modification. Separate MS analyses were performed on the Q-Exactive Plus instrument using parallel reaction monitoring (PRM) selecting for specific ^{12}C ions of ApoA-IV peptides p.18-43, p.19-43, and p.20-43 (MH_3^{3+} *m/z* 944.121, 892.087, and 868.408, respectively). Data have been recorded in a separate proteomics database; in January 2021, this database contained ~2100 clinical entries excluding controls, external research samples, and fats following decellularisation treatment [35].

ApoA-IV immunoprecipitation

ApoA-IV protein was immunoprecipitated from serum collected from three ApoA-IV patients (#1, #3, and #11) and

Table 1. Identification of the signal-containing peptides in FFPE clinical tissues.

#	Tissue	ApoA-IV score	Match/ USP	p.18–43	p.19–43	p.20–43	p.21–43	Notes
				^{18}ARAEVSADQVATVMWDYFSQLSNNA^{43}K				
1	Cardiac	8120	167/29	Y	Y	Y	Y	
2	Cardiac	6414	130/22	Y	Y	Y	Y	
3	Cardiac	4517	121/23	–	Y	Y	Y	Serum +ve for signal
4	Cardiac	3287	103/34	–	Y	Y	Y	
5	Cardiac	2686	78/16	–	–	–	Y	
6	Cardiac	2075	73/10	–	–	–	Y	
7	Cardiac	1591	47/10	–	–	–	Y	
8	Cardiac	1230	43/26	–	Y	Y	Y	
9	Cardiac	333	12/10	–	–	–	–	
10	Renal	8127	272/25	Y	Y	Y	Y	
11	Renal	4162	130/17	–	–	Y	Y	
12	Renal	3817	116/21	–	Y	Y	Y	
13	Renal	2079	60/14	–	–	Y	Y	
14	Renal	1789	42/21	–	–	–	Y	
15	Renal	825	32/11	–	–	Y	Y	
16	Duodenal	2361	87/22	–	–	–	Y	
17	Cardiac	10,176	332/33	–	Y	Y	Y	
18	Cardiac	7866	266/34	Y	Y	Y	Y	
19	Cardiac	7863	237/33	Y	Y	Y	Y	p.15-43 unconfirmed
20	Cardiac	2884	107/20	–	Y	Y	Y	ApoA-IV + TTR present
21	Renal	6226	136/13	–	Y	Y	Y	
22	Renal	6357	167/26	Y	Y	Y	Y	p.17-43 unconfirmed
23	Renal	883	16/7	–	–	–	–	
24	ENT	5996	188/31	–	Y	Y	Y	
25	Cardiac	4245	113/27	Y	Y	Y	Y	ApoA-IV + TTR present

Mascot score, significant mass spectra (spectral matches/unique significant peptides, USP). Further clinical details are shown in supplementary material, Table S1. Patients 1–15 attended the NAC clinic and were diagnosed with cardiac or renal ApoA-IV amyloidosis. Patient 16 attended the clinic with localised amyloid in the gut. FFPE blocks from patients 17–24 were received from other centres for histology review. The mature protein N-terminal peptide, p.21-43 (EVSADQVATVMWDYFSQLSNNAK) was present in 22/24 samples. Signal peptides were identified in 17/24 patient samples, with p.20-43 being the most common. Peptides p.15-43 and p.17-43 were not confirmed by co-elution with standards. The block from the original ApoA-IV patient (#25) from Sweden was retrieved and re-analysed; ApoA-IV signal peptides were present. Both TTR and ApoA-IV were identified in separate regions of the tissue from patients 20 and 25. ApoA-IV signal sequence was also present in a fat biopsy and a blood sample collected from patient 3.

from two healthy controls. A mouse monoclonal anti-human ApoA-IV antibody (Santa Cruz Biotechnology, Dallas, TX, USA) was buffer-exchanged into PBS using BioSpin columns (Bio-Rad Laboratories, Watford, UK) and incubated overnight with rotation at 4 °C with CNBR-activated Sepharose 4B beads (Sigma-Aldrich, St Louis, MO, USA). The antibody beads were used to immunoprecipitate ApoA-IV using the procedure described previously for TTR [34].

Fibrillogenesis of ApoA-IV peptides p.18-43, p.19-43, p.20-43, and p.21-43

Synthetic ApoA-IV peptides p.18-43, p.19-43, and p.20-43, and the N-terminal peptide p.21-43 (peptide purity > 95%) were purchased from Life Technologies Limited, Paisley, UK. They were dissolved at 200 μg/ml in phosphate-buffered saline (pH 7.4) containing 10 μM thioflavin T (ThT) and placed in Costar 96-well plates (Fisher Scientific, Loughborough, UK) in a BMG LABTECH, FLUOstar Omega double-orbital shaker (BMG LABTECH, Ortenberg, Germany). Three replicates for each peptide were incubated at 37 °C with shaking at 900 rpm, and ThT fluorescence (excitation at 440 nm, emission at 480 nm) was recorded for 24 h at 500 s intervals.

Transmission electron microscopy (TEM)

A drop of a suspension of fibrils, collected following 24 h incubation, was loaded onto a formvar/carbon-coated 300-mesh copper grid and excess solvent was allowed to dry at room temperature for 3 min before blotting with filter paper. After washing with water for 10 s, the dry sample was stained with 2% uranyl acetate solution for 1 min and examined in a JEOL JEM-1400 Flash transmission electron microscope (JEOL, Tokyo, Japan) operating at 120 kV.

Results

Cardiac ApoA-IV amyloidosis was initially diagnosed in nine patients (all male, median age 77 years), renal amyloidosis in six patients (five male and one female, median age 68 years), and duodenal ApoA-IV amyloidosis in a single patient, all attending clinics at the National Amyloidosis Centre (Table 1). All renal patients had previous chronic kidney disease, with amyloid deposition but with no plasma cell dyscrasia or clone noted. On ^{123}I SAP scintigraphy, no visceral amyloid deposits were detected. All patients went on to develop cardiac amyloid, from between 6 months and 7 years post-renal amyloid diagnosis. Cardiac amyloid

deposition was assessed using a Tc-DPD scan on all patients, all resulting in Perugini grade 0. A clinical summary is shown in supplementary material, Table S1. The morphology in the renal and cardiac cases was different but characteristic, in that amyloid presents as swathes of medullary sheets in renal biopsies and can be minimal in the cardiac tissue, with scanty deposits surrounding myocytes or in vessels. IHC indicated the presence of ApoA-IV in four cases, and also in a separate, non-cardiac biopsy from patient 8. Other samples were not tested with the ApoA-IV antibody. There was no evidence for ApoA-IV immunostaining in any non-ApoA-IV amyloid despite high ApoA-IV Mascot scores. In each case, ApoA-IV was identified by proteomics as the top scoring protein together with a low probability for the presence of other candidate amyloid proteins. The Mascot scores, which use a probability-based algorithm, were high: in only one sample was the score less than 800, which is ten times the minimum score of 80 used in our algorithm to confidently identify proteins. This is in agreement with the criteria originally reported by Dasari *et al* [26]. We re-examined the data in our clinical proteomics database for the presence of ApoA-IV amyloid using these criteria. ApoA-IV amyloid was identified in eight histology review samples from cardiac (4), renal (3), and oral mucosal (1) biopsies (#17–24). Distinct areas of TTR and ApoA-IV were observed by both IHC and proteomics in #20. In each of these additional cases, ApoA-IV was the top scoring (highest probability) amyloid protein, with 7/8 scoring greater than 2400, which is 30-fold higher than the minimum acceptable score. With the exception of fibrinogen Aα and ApoA-I, which can be excluded by other criteria [32], there were no other amyloid candidates present. Clinical and morphological data, where available, were consistent with the diagnosis. These data are summarised in Table 1 and Figure 1 and are also expressed as a Scaffold output (Proteome Software, Inc, Portland, OR, USA) in supplementary material, Figure S1. ApoA-IV was present with a minimum Mascot score of 80 in 55% (1142/2075) of the samples in our database where ApoA-IV was not identified as the amyloid type (supplementary material, Table S2). This is not unexpected as it is one of the three currently acknowledged amyloid signature proteins. It was the top scoring amyloid protein in only 311 samples, with high scores (>2400) observed in only eight (1.8%) of the samples (supplementary material, Table S2 and Figure 1). Of the uncertain diagnoses with a top ApoA-IV score, only 16 showed no evidence for other amyloid proteins; the ApoA-IV scores were relatively low (82–383) and there was no other reason to consider ApoA-IV as the amyloid protein.

During the analyses of the clinical and histology review ApoA-IV cases, we observed that the tryptic peptide p.20-43 (AEVSADQVATVMWDYFSQLSNNAK) was

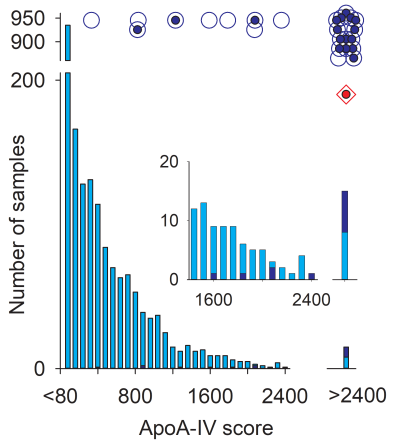

Figure 1. The ApoA-IV Mascot score histogram for all samples (light blue bars); the histogram for ApoA-IV clinical amyloid samples is shown as dark blue bars. The scores of the 24 clinical ApoA-IV patients are also shown as open blue circles together with that of the original Swedish sample (open diamond); in each of these cases, ApoA-IV was the top scoring amyloid protein. Signal sequence was detected in 17/24 samples (closed blue circles) and also in the Swedish sample (closed red circle in diamond).

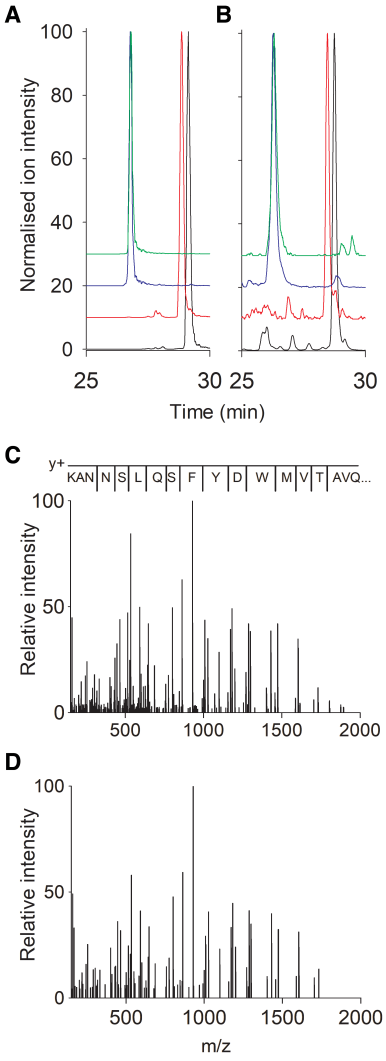

Figure 2. Normalised ion chromatograms (MH_3^{3+}) for the signal-containing peptides p.18-43, p.19-43, and p.20-43, together with the N-terminal peptide p.21-43 for (A) authentic standards and (B) patient 11. (C, D) MSMS spectra (MH_3^{3+}) for the p.18-43 standard and patient 11. The common y ion series (y3–y15) is highlighted.

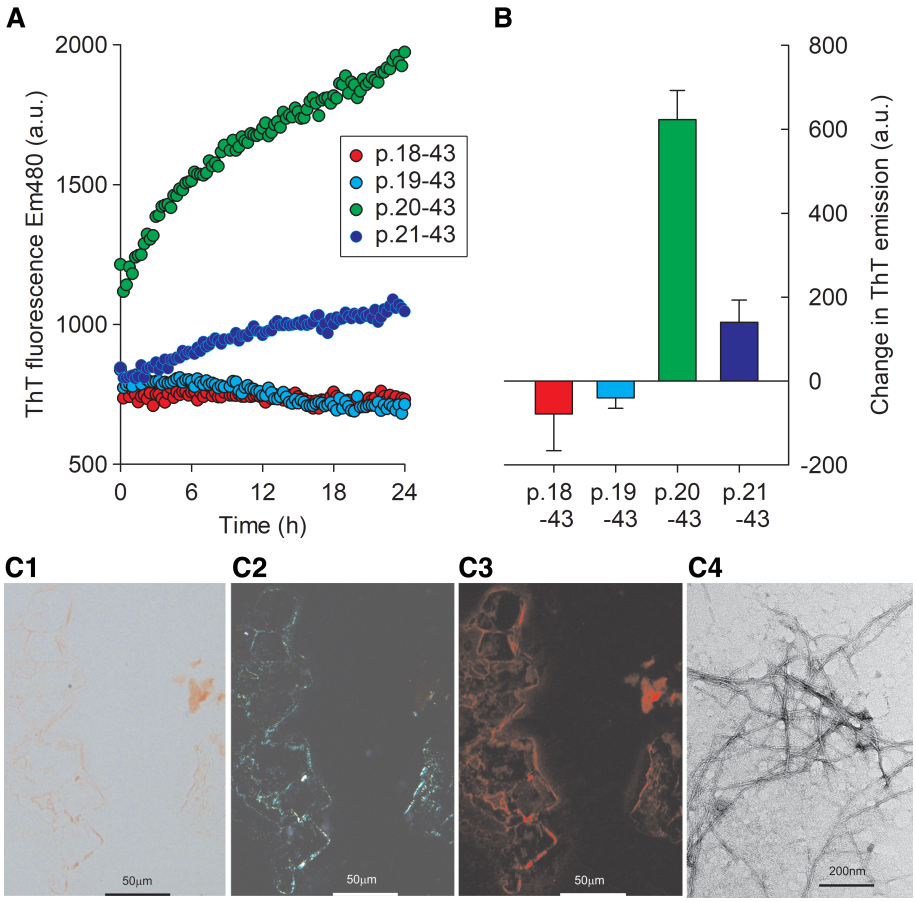

Figure 3. (A) Fibrillogenesis at pH 7 and 37 °C of the signal-containing peptides p.18-43, p.19-43, and p.20-43, and the N-terminal peptide p.21-43 analysed at the same time. (B) Three separate experiments were performed for each peptide, and the mean (SD) of the change in ThT fluorescence emission between 0.25 and 18 h is shown. Fluorescence intensity is shown in arbitrary units (a.u.). Panels C1–C4 show the bright field Congo red staining for the p.20-43 fibrils together with the fluorescence with and without the polarising filter, and the electron micrograph of the p.20-43 fibrils (after 24 h of incubation).

detected in 17/24 cases. This was unexpected as it corresponds to a tryptic cleavage after p.20R in the signal region. The raw data were reanalysed by Mascot using semi-trypsin as the *in silico* protease: additional signal-containing peptides were observed corresponding to p.18-43 (ARAEVSA…, $n = 6$) and p.19-43 (RAEVSA… $n = 12$), together with single examples of p.17-43 (GARAEVSA…) and p.15-43 (VAGARAEVSA…). Signal-containing peptides were present in a post-mortem sample from a presumed cardiac TTR patient (#20) where distinct areas of both ApoA-IV and TTR immunostaining were observed (Table 1). The N-terminal peptide p.21-43 (EVSA…) was present in 22/24 samples. There were also some examples of truncated N-terminal peptides p.22-43 (VSA…) and p.23-43 (SA…), but none without the expected p.43 lysine C-terminus which is generated by trypsin in the sample workup. This indicated that ApoA-IV amyloid was associated with the presence of signal sequence. A single signal peptide, p.19-43, was also identified in a fat sample, from patient 3, which had been treated by the decellularisation method designed to remove non-amyloid deposits and enhance proteomic identification [35]. As controls, all other non-ApoA-IV samples with an ApoA-IV score greater than 800 were examined ($n = 266$); the N-terminal peptide (p.21-43) was present in 27% of samples; however, only a single sample of fat showed evidence of p.18-43, and this was identified from a single MSMS spectrum. The protein coverage of ApoA-IV for the ApoA-IV patients and controls with high ApoA-IV signature scores is shown in supplementary material, Figure S2. This indicates that ApoA-IV amyloid is also associated with a reduced C-terminal load.

The FFPE block of cardiac tissue from the original Swedish patient (#25) diagnosed with ApoA-IV amyloidosis was obtained, and sections were recut and analysed by histochemistry: distinct areas were observed exhibiting ApoA-IV and TTR immunoreactivity, respectively, in agreement with the original data. Two areas of each immuno-positive region were laser-dissected and prepared for proteomics using our standard procedure. In the ApoA-IV-positive section, proteomics identified ApoA-IV as the top scoring protein (Mascot scores 4245 and 2547), together with the signature proteins SAP and ApoE. Other lower scoring (score < 750) proteins were also observed including TTR, ApoA-I, and kappa light chain. Three signal-containing ApoA-IV peptides, p.18-43, p.19-43, and p.20-43, were present together with the N-terminal peptide p.21-43. In the TTR immuno-positive area, TTR was

the top scoring protein (2753 and 2000); ApoA-IV was present with lower scores (<600) and there was no evidence for signal peptides, which is consistent with ApoA-IV in this region being a co-deposited signature protein.

To confirm the identity of these Mascot-identified signal-containing peptides, four authentic peptide samples (p.18-, p.19-, p.20-, and p.21-43) were analysed under our standard LCMS conditions. Peptides p.15-43 and p.17-43 were not compared against standards and their identity is based on Mascot search analysis only. Peptides p.18-43 and p.19-43 essentially co-eluted at 26.8 min, with p.20-43 and the N-terminal peptide p.21-43 eluting later at 28.8 and 29.1 min, respectively. Each peptide generated a similar set of y ions (y3–y15) together with characteristic b ions. The clinical ApoA-IV samples and the Swedish cardiac sample showed the same relative retention times and elution pattern as the standards (Figure 2), and generated similar MSMS spectra (supplementary material, Figure S3). These data confirm that there is a signal-containing protein in ApoA-IV amyloid.

Since any ApoA-IV deposited in amyloid must have come from the circulation, serum from patients 1, 3, and 11, whose samples showed high ApoA-IV scores, was immunoprecipitated with anti-ApoA-IV antiserum and the sample was subjected to PRM mass spectrometric analysis targeting the signal peptides p.18-43, p.19-43, and p.20-43. All three peptides were present only in the immunoprecipitate from patient 3 (supplementary material, Figure S4), although none were identified in the remaining two ApoA-IV patients, or in serum from two healthy controls. These data are consistent with a very low normal circulating concentration of signal-containing proteins.

To determine whether these additional signal residues could influence the deposition of amyloid, the authentic peptides were incubated in PBS buffer at 37 °C with gentle shaking, and fibril formation was measured by ThT fluorescence emission as previously described [36]. Although neither of the arginine-containing signal peptides (p.18-43 and p.19-43) showed any fibril formation, the most common signal-containing peptide, p.20-43, and to a much lesser extent the N-terminal peptide p.21-43 were fibrillogenic under these mild conditions (Figure 3). The fibrils from the p.20-43 peptide exhibited the classic amyloid green birefringence following Congo red staining, and the electron micrographs were consistent with amyloid fibrils. Small specks of positive material could also be observed for the p.21-43 (N-terminal peptide) preparation; however, there was no evidence for amyloid fibrils in the incubates of p.18-43 and p.19-43. The addition of a single alanine to the normal N-terminal peptide, p.21-43, has markedly increased its fibrillogenicity; this effect is lost by further extension with arginine (p.18-43 and p.19-43).

Discussion

Mature ApoA-IV is a 376-residue (p.21-396) circulating protein that is involved in a number of physiological processes. ApoA-IV amyloid deposits were first recognised in a Swedish cardiac patient through traditional protein biochemistry analyses and the development of specific and complementary immunohistochemical methods [16]. The advent of diagnostic amyloid proteomics pioneered at the Mayo Clinic revolutionised the field and made it possible to rapidly type amyloid [37,38]. ApoA-IV is a common constituent of amyloid tissue; therefore its identification alone is insufficient to identify the amyloid protein: here, the proteomics criteria identified by the Mayo Clinic, using an abnormally high number of ApoA-IV spectra coupled with the absence of other amyloid proteins, are central to confirming ApoA-IV amyloid. In our centre, we use the Mascot protein database search engine, which generates a probability-based score dependent on the quality and number of individual mass spectra to identify proteins (http://matrixscience.com). Although it is not a quantitative measure, the score is a surrogate for protein amount and is helpful in distinguishing the amyloid protein from contaminants. Our algorithm identifies ApoA-IV where it is the top scoring protein, normally with scores in excess of 1000, in the absence of other candidate amyloid proteins. Whilst our data are in general agreement with those of the Mayo Clinic, we note that a low score (or low total spectral count) does not preclude the presence of ApoA-IV amyloid. Equally, the absence of other amyloid proteins may be insufficient to distinguish ApoA-IV amyloid from the amyloid signature. Here, additional clinical, morphological/IHC, and proteomics features will increase confidence in the amyloid typing, and these were applied to identify 24 examples of ApoA-IV amyloid amongst over 2000 clinical samples in our current proteomics database. The presence of distinct areas of ApoA-IV and TTR amyloid in patient 20 is consistent with a diagnosis of two unrelated forms of amyloidosis: ApoA-IV together with age-related wild-type cardiac ATTR amyloidosis; this was also observed in the original Swedish sample [17].

The most unexpected finding of our study was the identification of signal sequence-containing peptides p.15-43, p.17-43, p.18-43, p.19-43, and, most commonly, p.20-43 in ApoA-IV amyloid deposits. Some of these peptides have previously been identified in a number of top-down proteomics analyses, for example in cerebrospinal fluid [39] and breast cancer tissue [40], although no biological role was ascribed. There was also evidence for p.20-43 in the first proteomics identification of renal ApoA-IV report from the Mayo Clinic, where residue p.20A was highlighted as an identified tryptic peptide, although its appearance did not receive any comment [26]. At least one signal peptide was present in 17/24 of the ApoA-IV amyloid cases, as well as in the original Swedish cardiac sample. The identity of the three main signal peptides, p.18-43, p.19-43, and p.20-43, in patient-derived samples was confirmed by chromatographic and mass spectrometric comparison with authentic peptides and does not rely simply on a Mascot-generated identification. ApoA-IV is a circulating protein that is synthesised in the intestine; therefore it, and the associated signal-containing proteins present in amyloid, should arise from the blood. Using targeted

PRM analysis, we could identify all three signal peptides present in blood of patient 3, although none were detected in two other patients or in two healthy controls. This would indicate that signal-containing proteins are not a major component of circulating ApoA-IV. The signal does not appear to be associated with signature ApoA-IV as only a single poor-quality signal peptide was found in only one of the 266 non-ApoA-IV cases with high scores (>800) examined. It was not possible in the current study to determine whether the signal-containing peptides identified in amyloid and in blood are part of the full protein or a smaller truncated protein; however, the limited coverage data would suggest that the amyloidogenic ApoA-IV contains a lower proportion of C-terminal protein than signature ApoA-IV.

The major circulating form of ApoA-IV (p.147N) is inherently amyloidogenic [16], and so the presence of signal residues in ApoA-IV amyloid could simply be due to an increased circulating concentration. This could be caused by faulty processing, or secondary effects of the additional signal sequence whereby altered lipid binding could raise the free protein plasma concentration. Our *in vitro* fibrillogenesis data with peptides p.18-43 to p.21-43, showing that the addition of a single alanine residue to the normal N-terminus causes increased fibrillogenicity, raise the possibility that the presence of signal residues could exert a direct and deleterious effect on the circulating protein. This could be propagated through a number of mechanisms including direct destabilisation of the protein, altered binding to lipids and other proteins such as clusterin, or increased sensitivity to endogenous protease activity or mechanical forces [36,41,42].

Although there is a large gap between the behaviour of a small peptide *in vitro* and the stability of a protein in the complex milieu of blood, our data are suggestive of a potential causative relationship between the presence of signal sequence and enhanced ApoA-IV amyloidogenicity. It may be that the presence of these signal residues is no more than an additional marker that can be applied to increase confidence in ApoA-IV amyloid diagnosis; however, since ApoA-IV is involved in other human diseases [43], the presence of signal sequence in the circulating protein could have other deleterious pathophysiological effects.

Acknowledgements

The National Amyloidosis Centre is funded directly through NHS England. Core support for the Wolfson Drug Discovery Unit is provided by the UK National Institute for Health Research Biomedical Research Centre and Unit Funding scheme via the UCLH/University College London Biomedical Research Centre. Funding for the proteomics platform was generously provided by the Wolfson Foundation, Grant No PR/YLR/NW/20885, and the University College London Amyloidosis Research Fund. PW has received support from the Selander Foundation, Uppsala, Sweden.

Author contributions statement

GWT, DC, VB and JDG designed the study. GWT and DC analysed the data and wrote the paper. NBR, JAG and NB variously carried out the staining procedures, extraction (LCD), digestion, and mass spectrometric analyses of the samples. DC and PN carried out the immunoprecipitation and PRM analysis and, with GV and AM, undertook the fibrillogenesis studies. PN and PPM carried out electron microscopy; AC gave insight into structural analysis; SG and LM contributed to discussion and preliminary data. PW provided the original Swedish sample and advised on IHC analysis and ApoA-IV amyloidosis. JDG and PNH provided clinical interpretation, and DR advised on genetics. The clinical database algorithm was implemented and developed by AB. All the authors provided interpretative input and reviewed the manuscript.

Data availability statement

Anonymised raw mass spectra data, Mascot mgf files, and raw data of fibrillogenesis experiments are available on request from the corresponding author.

References

1. Pepys MB. Amyloidosis. *Annu Rev Med* 2006; **57:** 223–241.
2. Benson MD, Buxbaum JN, Eisenberg DS, *et al*. Amyloid nomenclature 2020: update and recommendations by the International Society of Amyloidosis (ISA) nomenclature committee. *Amyloid* 2020; **27:** 217–222.
3. Gillmore JD, Lachmann HJ, Rowczenio D, *et al*. Diagnosis, pathogenesis, treatment, and prognosis of hereditary fibrinogen A alpha-chain amyloidosis. *J Am Soc Nephrol* 2009; **20:** 444–451.
4. Galant NJ, Westermark P, Higaki JN, *et al*. Transthyretin amyloidosis: an under-recognized neuropathy and cardiomyopathy. *Clin Sci (Lond)* 2017; **131:** 395–409.
5. Falk RH, Alexander KM, Liao R, *et al*. AL (light-chain) cardiac amyloidosis: a review of diagnosis and therapy. *J Am Coll Cardiol* 2016; **68:** 1323–1341.
6. Merlini G. AL amyloidosis: from molecular mechanisms to targeted therapies. *Hematology Am Soc Hematol Educ Program* 2017; **2017:** 1–12.
7. Plante-Bordeneuve V. Transthyretin familial amyloid polyneuropathy: an update. *J Neurol* 2018; **265:** 976–983.
8. Mahmood S, Palladini G, Sanchorawala V, *et al*. Update on treatment of light chain amyloidosis. *Haematologica* 2014; **99:** 209–221.
9. Simons JP, Al-Shawi R, Ellmerich S, *et al*. Pathogenetic mechanisms of amyloid A amyloidosis. *Proc Natl Acad Sci U S A* 2013; **110:** 16115–16120.
10. Pepys MB, Hawkins PN, Booth DR, *et al*. Human lysozyme gene mutations cause hereditary systemic amyloidosis. *Nature* 1993; **362:** 553–557.
11. Saraiva MJ, Birken S, Costa PP, *et al*. Family studies of the genetic abnormality in transthyretin (prealbumin) in Portuguese patients with familial amyloidotic polyneuropathy. *Ann N Y Acad Sci* 1984; **435:** 86–100.
12. Benson MD, Liepnieks J, Uemichi T, *et al*. Hereditary renal amyloidosis associated with a mutant fibrinogen alpha-chain. *Nat Genet* 1993; **3:** 252–255.

13. Westermark P, Sletten K, Johansson B, *et al*. Fibril in senile systemic amyloidosis is derived from normal transthyretin. *Proc Natl Acad Sci U S A* 1990; **87:** 2843–2845.
14. Mohammed SF, Mirzoyev SA, Edwards WD, *et al*. Left ventricular amyloid deposition in patients with heart failure and preserved ejection fraction. *JACC Heart Fail* 2014; **2:** 113–122.
15. Zhao L, Buxbaum JN, Reixach N. Age-related oxidative modifications of transthyretin modulate its amyloidogenicity. *Biochemistry* 2013; **52:** 1913–1926.
16. Bergström J, Murphy C, Eulitz M, *et al*. Codeposition of apolipoprotein A-IV and transthyretin in senile systemic (ATTR) amyloidosis. *Biochem Biophys Res Commun* 2001; **285:** 903–908.
17. Bergström J, Murphy CL, Weiss DT, *et al*. Two different types of amyloid deposits – apolipoprotein A-IV and transthyretin – in a patient with systemic amyloidosis. *Lab Invest* 2004; **84:** 981–988.
18. Hood BL, Conrads TP, Veenstra TD. Mass spectrometric analysis of formalin-fixed paraffin-embedded tissue: unlocking the proteome within. *Proteomics* 2006; **6:** 4106–4114.
19. Palmer-Toy DE, Krastins B, Sarracino DA, *et al*. Efficient method for the proteomic analysis of fixed and embedded tissues. *J Proteome Res* 2005; **4:** 2404–2411.
20. Murphy CL, Wang S, Williams T, *et al*. Characterization of systemic amyloid deposits by mass spectrometry. *Methods Enzymol* 2006; **412:** 48–62.
21. Rodriguez FJ, Gamez JD, Vrana JA, *et al*. Immunoglobulin derived depositions in the nervous system: novel mass spectrometry application for protein characterization in formalin-fixed tissues. *Lab Invest* 2008; **88:** 1024–1037.
22. Dogan A. Amyloidosis: insights from proteomics. *Annu Rev Pathol* 2017; **12:** 277–304.
23. Theis JD, Dasari S, Vrana JA, *et al*. Shotgun-proteomics-based clinical testing for diagnosis and classification of amyloidosis. *J Mass Spectrom* 2013; **48:** 1067–1077.
24. Vrana JA, Gamez JD, Madden BJ, *et al*. Classification of amyloidosis by laser microdissection and mass spectrometry-based proteomic analysis in clinical biopsy specimens. *Blood* 2009; **114:** 4957–4959.
25. Dasari S, Theis JD, Vrana JA, *et al*. Amyloid typing by mass spectrometry in clinical practice: a comprehensive review of 16,175 samples. *Mayo Clin Proc* 2020; **95:** 1852–1864.
26. Dasari S, Amin MS, Kurtin PJ, *et al*. Clinical, biopsy, and mass spectrometry characteristics of renal apolipoprotein A-IV amyloidosis. *Kidney Int* 2016; **90:** 658–664.
27. Said SM, Sethi S, Valeri AM, *et al*. Renal amyloidosis: origin and clinicopathologic correlations of 474 recent cases. *Clin J Am Soc Nephrol* 2013; **8:** 1515–1523.
28. Sethi S, Theis JD, Shiller SM, *et al*. Medullary amyloidosis associated with apolipoprotein A-IV deposition. *Kidney Int* 2012; **81:** 201–206.
29. Bois MC, Dasari S, Mills JR, *et al*. Apolipoprotein A-IV-associated cardiac amyloidosis. *J Am Coll Cardiol* 2017; **69:** 2248–2249.
30. Gilbertson JA, Hunt T, Hawkins PN. Amyloid typing: experience from a large referral centre. In *Amyloid and Related Disorders*, Picken MM, Dogan A, Herrera GA (eds). Humana Press: Totowa, NJ, 2012; 231–238.
31. Gilbertson JA, Theis JD, Vrana JA, *et al*. A comparison of immunohistochemistry and mass spectrometry for determining the amyloid fibril protein from formalin-fixed biopsy tissue. *J Clin Pathol* 2015; **68:** 314–317.
32. Canetti D, Rendell NB, Gilbertson JA, *et al*. Diagnostic amyloid proteomics: experience of the UK National Amyloidosis Centre. *Clin Chem Lab Med* 2020; **58:** 948–957.
33. Westermark GT, Ihse E, Westermark P. Development of mouse monoclonal antibodies against human amyloid fibril proteins for diagnostic and research purposes. *Methods Mol Biol* 2018; **1779:** 401–414.
34. Canetti D, Rendell NB, Di Vagno L, *et al*. Misidentification of transthyretin and immunoglobulin variants by proteomics due to methyl lysine formation in formalin-fixed paraffin-embedded amyloid tissue. *Amyloid* 2017; **24:** 233–241.
35. Mangione PP, Mazza G, Gilbertson JA, *et al*. Increasing the accuracy of proteomic typing by decellularisation of amyloid tissue biopsies. *J Proteomics* 2017; **165:** 113–118.
36. Marcoux J, Mangione PP, Porcari R, *et al*. A novel mechano-enzymatic cleavage mechanism underlies transthyretin amyloidogenesis. *EMBO Mol Med* 2015; **7:** 1337–1349.
37. Tasaki M, Ueda M, Hoshii Y, *et al*. A novel age-related venous amyloidosis derived from EGF-containing fibulin-like extracellular matrix protein 1. *J Pathol* 2019; **247:** 444–455.
38. Sethi S, Dasari S, Plaisier E, *et al*. Apolipoprotein CII amyloidosis associated with p.Lys41Thr mutation. *Kidney Int Rep* 2018; **3:** 1193–1201.
39. Guldbrandsen A, Vethe H, Farag Y, *et al*. In-depth characterization of the cerebrospinal fluid (CSF) proteome displayed through the CSF proteome resource (CSF-PR). *Mol Cell Proteomics* 2014; **13:** 3152–3163.
40. Shen Y, Tolić N, Liu T, *et al*. Blood peptidome-degradome profile of breast cancer. *PLoS One* 2010; **5:** e13133.
41. Mangione PP, Esposito G, Relini A, *et al*. Structure, folding dynamics, and amyloidogenesis of D76N β2-microglobulin: roles of shear flow, hydrophobic surfaces, and α-crystallin. *J Biol Chem* 2013; **288:** 30917–30930.
42. Lavatelli F, Mazzini G, Ricagno S, *et al*. Mass spectrometry characterization of light chain fragmentation sites in cardiac AL amyloidosis: insights into the timing of proteolysis. *J Biol Chem* 2020; **295:** 16572–16584.
43. Qu J, Ko CW, Tso P, *et al*. Apolipoprotein A-IV: a multifunctional protein involved in protection against atherosclerosis and diabetes. *Cells* 2019; **8:** 319.

SUPPLEMENTARY MATERIAL ONLINE

Figure S1. Scaffold readout of the top scoring proteins in each of the 24 ApoA-IV clinical samples and the original Swedish sample (#25)

Figure S2. ApoA-IV protein coverage by proteomics

Figure S3. Comparison of MSMS spectra from the original Swedish ApoA-IV sample with authentic standards

Figure S4. MSMS spectra for p.18-43, 19-43, and 20-43 obtained following immunoprecipitation of ApoA-IV from the serum of patient 3 and analysis by PRM

Table S1. Clinical details of the 16 patients attending the NAC clinics who were identified with ApoA-IV amyloidosis

Table S2. Amyloid type determined in patient samples analysed by proteomics (April 2016–early January 2021), excluding controls and some research samples